Effect of Prior Austenite Grain Size on the Morphology of Nano-Bainitic Steels

KRITIKA SINGH, AVANISH KUMAR, and APARNA SINGH

The strength in nanostructured bainitic steels primarily arises from the fine platelets of bainitic ferrite embedded in carbon-enriched austenite. However, the toughness is dictated by the shape and volume fraction of the retained austenite. Therefore, the exact determination of processing–morphology relationships is necessary to design stronger and tougher bainite. In the current study, the morphology of bainitic ferrite in Fe-0.89C-1.59Si-1.65Mn-0.37Mo-1-Co-0.56Al-0.19Cr (wt pct) bainitic steel has been investigated as a function of the prior austenite grain size (AGS). Specimens were austenitized at different temperatures ranging from 900 °C to 1150 °C followed by isothermal transformation at 300 °C. Detailed microstructural characterization has been carried out using scanning electron microscopy and X-ray diffraction. The results showed that the bainitic laths transformed in coarse austenite grains are finer resulting in higher hardness, whereas smaller austenite grains lead to the formation of thicker bainitic laths with a large fraction of blocky type retained austenite resulting in lower hardness.

I. INTRODUCTION

NANOSTRUCTURED bainitic steels consist of slender plates of ferrite of thickness less than 100 nm[1–5] with carbon-enriched retained austenite. Extremely high hardness has been reported in these steels since the numerous ferrite austenite interfaces block dislocation motion effectively thus reducing the mean free path for dislocation glide.[1,6] This unique microstructure is achieved due to growth by displacive transformation during prolonged isothermal treatments at temperatures as low as 125 to 300 °C.[6–9] In addition to the transformation temperature, prior austenite grain size (AGS) can potentially impact the mechanical properties of nano-bainite (NB) by impacting the kinetics of transformation and hence the resulting microstructure.

There have been a limited number of investigations on leveraging the prior AGS to control the kinetics and morphology of NB steels. Matsuzaki et al.[10] studied the effect of AGS on the overall kinetics of bainite transformation in a low as well as a high carbon bainitic steel. It was concluded that refinement of prior AGS leads to an acceleration of the rate of transformation when the overall reaction is limited by a slow growth rate. However, for nucleation-limited kinetics, AGS refinement slows down the transformation to bainite. Hu et al.[11] have shown a mild increase in the transformation kinetics of Fe-0.95C-0.91-Si-1.30Mn-2.30Cr-0.99Mo-0.17Ti nano-bainite with an increase in AGS and have attributed it to unhindered growth of the sheaves in a larger grained steel. On the contrary, Jiang et al.[12] have shown that a decrease in prior AGS from 53 μm to 3 μm led to acceleration of bainitic transformation significantly. However, when the prior austenite had a grain size of 3 μm, more than 50 pct of the bainite was not nano-structured and was surrounded with chunky blocks of austenite resulting in poor impact toughness. In another study by Yuan et al.,[13] it was reported that the decrease in prior AGS increases incubation time for bainite nucleation which was confirmed by the shifting of nose of the C-curve towards the right. The limited number of studies done to elucidate the effect of prior AGS on bainite transformation clearly show that the prior AGS not only impacts the kinetics of bainite formation but can also affect the morphology of the bainitic sheaves formed and hence the resulting mechanical behavior. However, in most of the previous studies, the isothermal treatment for NB nucleation and growth has not been done for sufficient time to completely transform austenite to the fraction of NB determined by the $T_0^{'}$ line.[14] Hence, the dependence of final bainitic lath morphology on AGS remains unknown. That is a significant impediment to designing structural nano-bainitic steels since the microstructure is the key determinant of mechanical and corrosion properties.

KRITIKA SINGH, AVANISH KUMAR, and APARNA SINGH are with the Department of Metallurgical Engineering and Materials Science, Indian Institute of Technology Bombay, Mumbai, 400076, India. Contact e-mail: aparna_s@iitb.ac.in

In the current study, we have prepared NB steel specimens that have been austenitized at six different temperatures to get a range of prior AGS. All specimens have been isothermally held at 300 °C for sufficient time till no more transformation was observed. Therefore, the fraction of retained austenite is almost the same in all of the specimens. However, bainitic lath thickness and fraction of blocky retained austenite have been found to increase with a decrease in prior AGS resulting in degradation of hardness.

II. EXPERIMENTAL PROCEDURE

The steel investigated in the present study was produced in an induction furnace and was cast as an ingot with dimensions $140 \times 70 \times 60$ mm^3. The chemical composition of the alloy was determined using optical emission spectroscopy and is mentioned in Table I.

The ingot was subsequently homogenized at 1200 °C for 48 hours to eliminate any micro-segregation. Subsequently, the ingot was forged and rolled at 900 °C in multiple steps to a final thickness of 24 mm. Multiple specimens of dimensions 10 mm length and 4×4 mm^2 cross section were cut using an electric discharge machine. Specimens with different AGS were prepared by austenitizing at temperatures 1150 °C, 1100 °C, 1050 °C, 1000 °C, 950 °C, and 900 °C, respectively, for 15 to 25 minutes followed by isothermal holding at 300 °C for 8 hours in a BAHR DIL 805 dilatometer. A schematic of the heat treatment cycle is shown in Figure 1(a).

The cooling rate from austenitization temperature to isothermal transformation temperature (300 °C) was maintained at 100 °C/s by blowing helium gas to suppress pearlitic transformation. Figure 1 (b) shows the dilatation curves for isothermal holding at 300 °C after quenching from different austenitization temperatures. The dilatation strain was measured during the formation of bainite and hence can be a representation of reaction kinetics. It can be seen from Figure 1(b) that the dilatation curve saturates exhibiting the completion of bainitic transformation at 300 °C. An indirect method was adopted to form pro-eutectoid cementite along the austenite grain boundaries for different austenitization temperature to estimate PAGS as prior austenite grain boundaries were not visible in an optical or electron micrograph.[15], Specimens were ground on successive grades of SiC paper, starting from 400 grit to 2500 grit paper followed by final polishing using 0.5 μm size diamond paste and etched by alkaline sodium picrate. The prior AGS for all the specimens was measured using line intercept method from multiple images taken using OLYMPUS optical microscope.

Polished specimens of as transformed steels were etched by 2 pct Nital solution before detailed characterization using AURIGA ZEISS dual beam scanning electron microscope (SEM). The average bainitic lath thickness was measured by the intercept method from multiple SEM images for each specimen. Since the measurements were taken on random sections, stereological corrections were made to obtain the true bainitic lath thickness. Test lines were drawn perpendicular to the long edges i.e., in the shortest direction to obtain mean intercept $\overline{L}_T$. True average thickness, t is obtained by applying the relation $t = 2\overline{L}_T/\pi$.[16] There are two types of retained austenite based on its size in the microstructure i.e., blocky and film type. The volume fraction of different types of retained austenite were measured using point count method from the SEM micrographs.

X-ray diffraction (XRD) patterns of all the specimens were obtained using PANalytical X'pert Pro MPD system with Cu-K$_\alpha$ radiation. The XRD patterns were analyzed using X'Pert Highscore software and volume fraction of bainite and retained austenite were calculated using direct comparison method[17] from integrated intensities of (110), (200), (211), (220) ferrite peaks and (111), (200), (220), (311) austenite peaks, respectively.

The hardness of the specimens was measured using a Vickers micro-hardness tester at a load of 1 kgf with a dwell time of 10 s. The hardness values reported are an average of at least 15 indentations taken at various locations sufficiently apart from each other to avoid interaction effects. The error bars shown in the present work represent standard deviation unless otherwise stated.

III. RESULTS

Figure 2 shows the optical images of steels which were quenched from different austenitization temperature to a temperature just above A_{cm} line and allowed to form pro-eutectoid cementite along the boundaries of prior austenite. It is very clear from the optical images that prior AGS decreases with decrease in austenitization temperature.

Figure 3 shows the quantitative measurement of prior AGS as a function of austenitization temperature. It is clear that AGS decreases monotonically with decrease in austenitization temperature. The AGS varies from 108 to 21 μm when the austenitization temperature was reduced from 1150 °C to 900 °C respectively. An abrupt increase in prior AGS was observed when austenitization temperature was increased from 1050 °C to 1100 °C. The thermodynamic calculation was done using Thermo-Calc 2016b software package based on CALPHAD (Computer Coupling of Phase Diagrams

Table I. Chemical composition of the steel produced in the induction-melting furnace

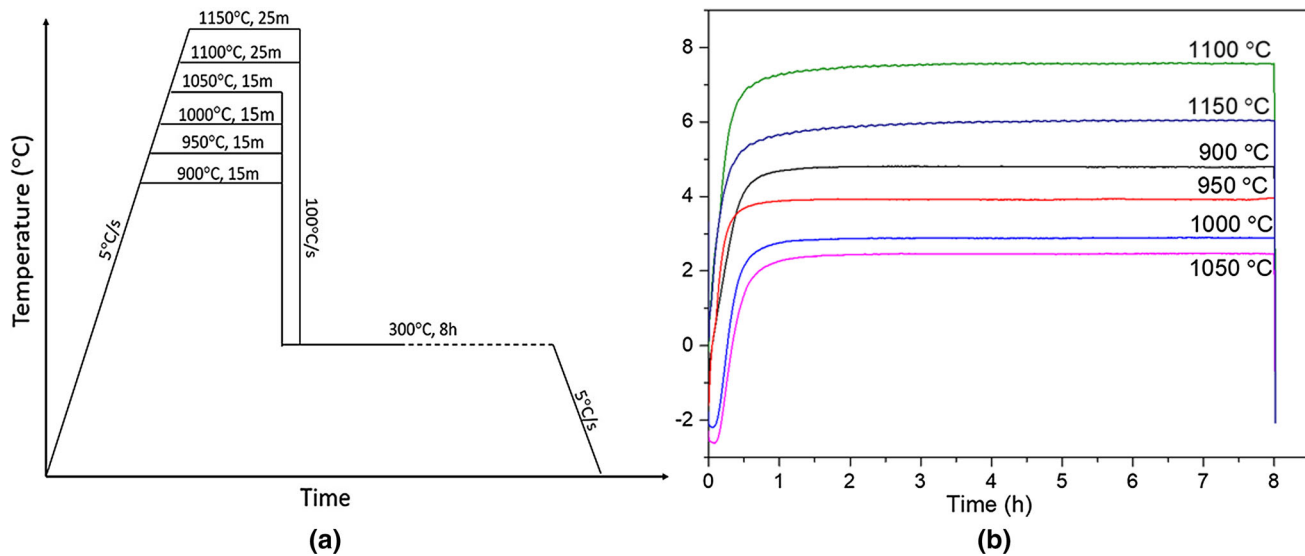| C	Si	Mn	Al	Co	Mo	Cr	Fe
0.89	1.59	1.56	0.56	1.0	0.37	0.19	rest

Fig. 1—(a) Schematic of the heat treatment cycle for bainitic transformation. (b) Dilatation curve for isothermal treatment after cooling from different austenitization temperatures.
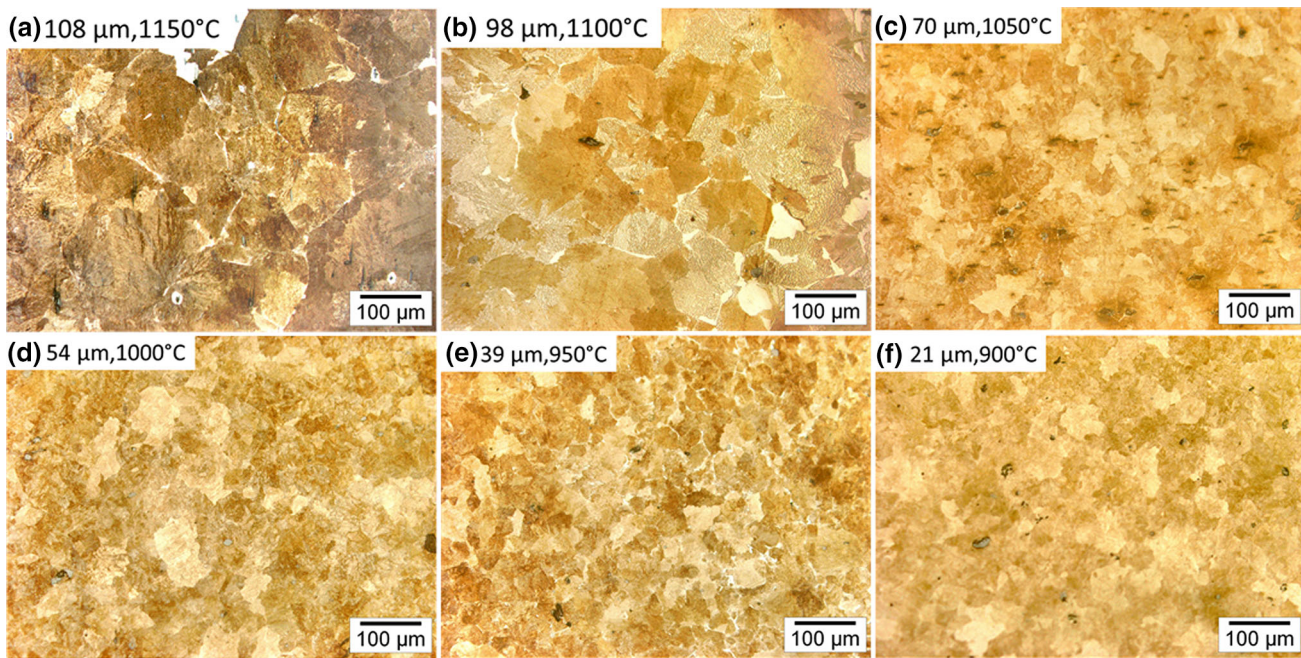

Fig. 2—Optical micrographs used for determining the prior AGS (a) 1150 °C, (b) 1100 °C, (c) 1050 °C, (d) 1000 °C, (e) 950 °C, and (f) 900 °C. Pro-eutectoid (white network) cementite is observed at the grain boundaries.

and Thermochemistry) to find out the change in phase fraction with temperature and it was found that AlN dissolves at 1088 °C. It is possible that these AlN particles were restricting the grain growth for temperature below 1088 °C and dissolution of these particles caused unrestricted growth of austenite.

X-ray diffraction patterns of all the specimens are shown in Figure 4. Peaks corresponding to ferrite and austenite are indexed based on respective (h k l) planes of phases. No cementite peaks were detected in XRD patterns. Phase quantification was done using the XRD patterns to evaluate the amount of bainitic ferrite

formed in different prior AGS specimens. The volume fraction of bainite is almost the same (~ 0.73) for all the specimens as shown in Figure 5.

The SEM micrographs of isothermally treated specimens after austenitizing at different temperatures are shown in Figure 6. All the specimens contained two morphologies of retained austenite: as fine films between laths of bainite (≤ specimen lath thickness) and as blocky islands (> specimen lath thickness) between sheaves of bainite. The distinction between two morphologies, in present study, is done based on the respective bainitic lath thickness of specimen. With a
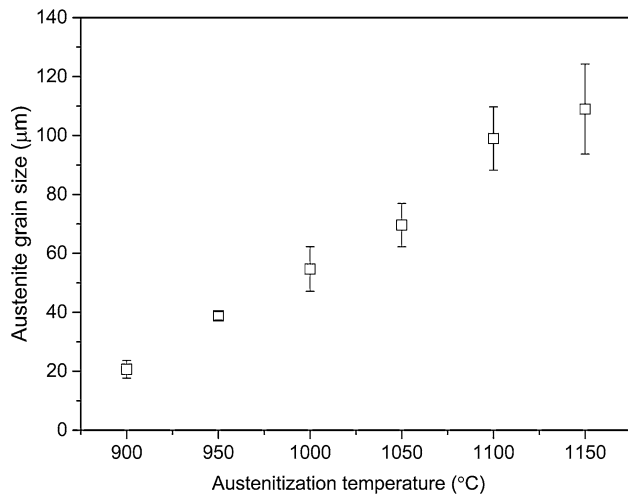
Fig. 3—Austenite grain size as a function of austenitization temperature.
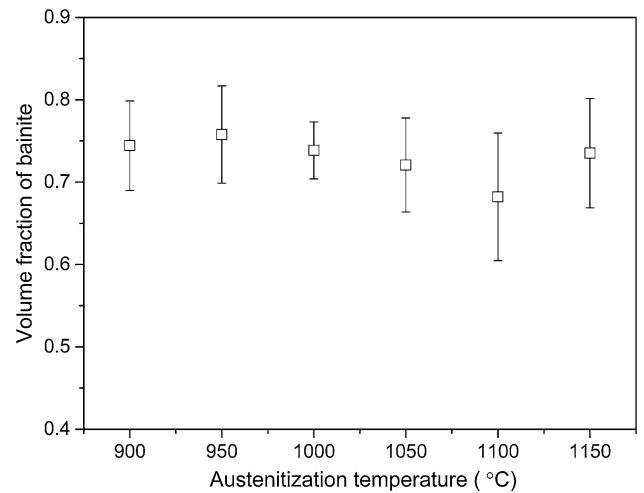

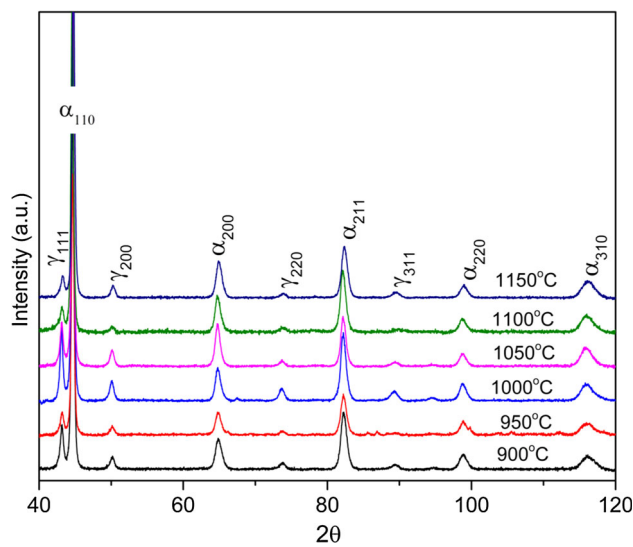Fig. 5—Volume fraction of bainite as a function of austenitization temperature.

Fig. 4—XRD plots for specimens treated at different austenitization temperature and held isothermally at 300 °C for 8 h.

decrease in AGS, morphology of both retained austenite and bainitic ferrite changes. Figures 6(a) through (d) shows long and thin laths with a significant amount of film type retained austenite in coarse prior AGS specimens. The finest bainitic lath is observed in specimen austenitized at 1000 °C (AGS: 54 μm) as seen in Figure 6(d). However, further decrease in AGS to 39 μm by prior austenitization at 950 °C causes thickening of bainitic laths as can be seen in Figure 6(e). The specimen austenitized at 900 °C (AGS: 21 μm) shows large amount of blocky austenite along with some austenite films between short and discontinuous bainitic laths as shown in Figure 6(f).

The percentage of film type retained austenite with prior AGS is deduced from the SEM micrographs and is shown in Figure 7. Although the volume fraction of retained austenite is same in all the specimens, percentage of film type of retained austenite is increased from 65 pct in specimen austenitized at 900 °C (AGS: 21 μm)

to 80 pct in specimen transformed at 1000 °C (AGS: 54 μm).

Figure 8 shows the hardness and bainitic lath thickness as a function of the prior AGS. It is can be seen that specimens with a prior AGS above 54 μm (austenitized at or above 1000 °C) show similar lath thickness of around 30 nm as well as similar hardness of around 5.3 GPa. However, with a decrease in prior AGS, hardness of the specimens decreases and laths become coarse. The specimen with the smallest AGS (austenitized at 900 °C) shows the highest lath thickness (~ 55 nm).

IV. DISCUSSION

Specimens with a range of austenite grain sizes were obtained by changing the austenitization temperature followed by isothermal transformation at a single temperature of 300 °C for 8 hours. During the isothermal heat treatment, dilatometric curve saturated for all the specimens indicating the completion of bainitic transformation. Hence, the bainitic volume fraction was almost the same for all the specimens (Figure 5) irrespective of the prior AGS since they were driven to transform under the same magnitude of chemical driving force.

Micrographs in Figure 6 clearly show that prior AGS has a significant effect on bainitic lath thickness. The nucleation and growth kinetics of bainite formation has been reported to be significantly impact by the prior AGS.[11,12,16] In the current study, the specimens of higher prior AGS show large fractions of film type retained austenite with finer bainitic laths. This thickening behavior of bainitic laths in smaller austenite grains is explained with the help of schematic diagram as shown in Figure 9. It shows the microstructural evolution of bainite laths with increasing time ($t_1 < t_2 < t_3$) in two different grain sizes of austenite. Since the isothermal transformation temperature is same for all the cases, chemical driving force for transformation, ΔG_{CHEM} is
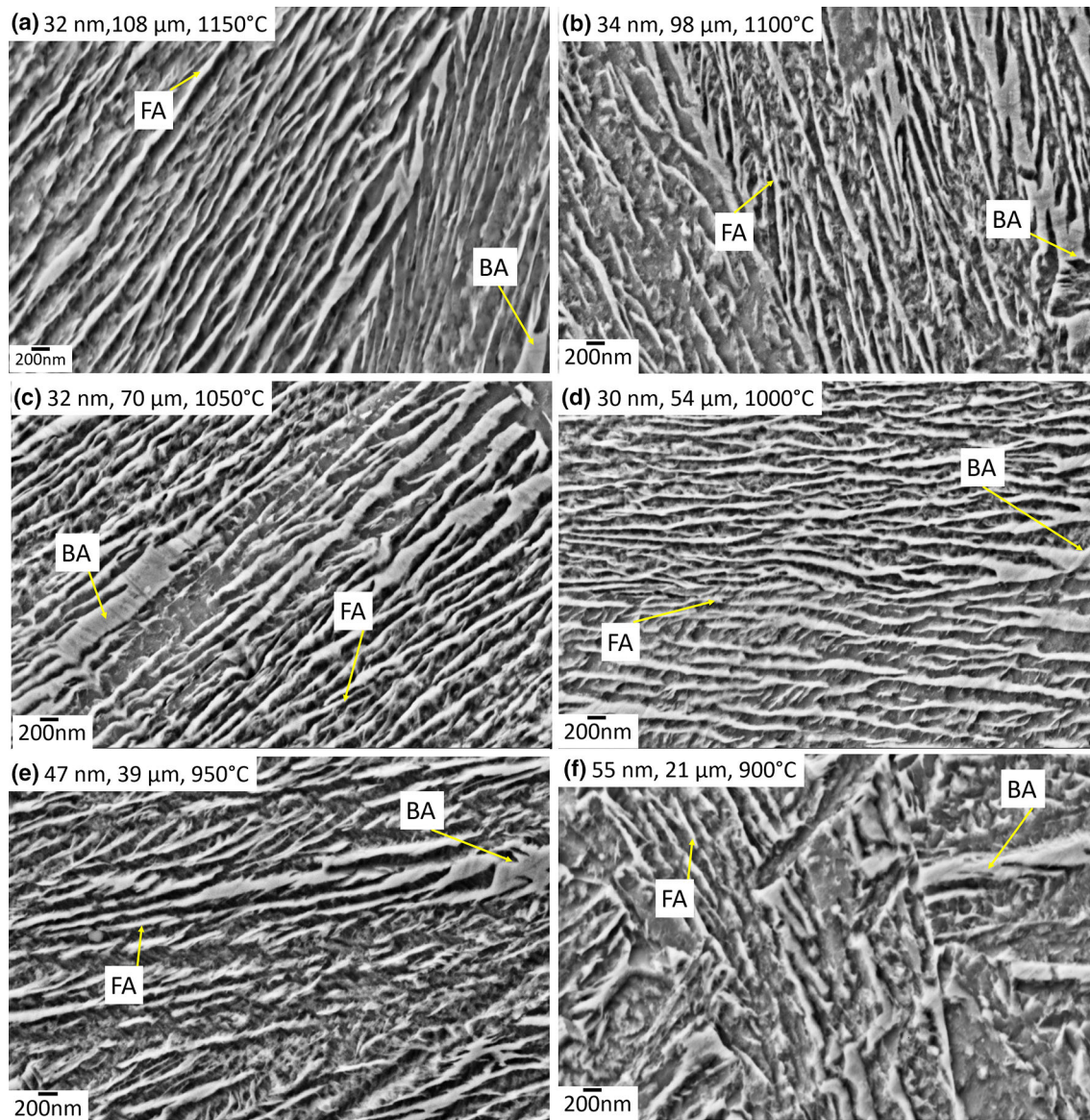
Fig. 6—SEM micrographs of isothermally treated specimens austenitized at (*a*) 1150 °C, (*b*) 1100 °C, (*c*) 1050 °C, (*d*) 1000 °C, (*e*) 950 °C, and (*f*) 900 °C showing bainite, film-like austenite (FA), and blocky austenite (BA). Labels on micrographs represent lath thickness, prior austenite grain size, and austenitization temperature, respectively.

same. Different crystallographic variants of bainite form from large density of nucleation sites in finer AGS specimens for high carbon steel as reported by T. Kaneshita *et al.*[18] Moreover, a decrease in austempering temperature further supports the formation of bainitic laths with multiple crystallographic variants.[19] As per the theory of bainitic transformation, a sub-unit of bainitic ferrite first nucleates at prior austenite grain boundary and lengthens till the capacity of untransformed austenite to accommodate plastic strain is exhausted. The newly formed sub-unit of bainitic ferrite which is supersaturated with carbon rejects its excess carbon to surrounding austenite. A new sub-unit then nucleates at the tip of already formed sub-unit of bainitic ferrite, and this way sheaf structure evolves.[20] The growth of bainitic plates can also be impeded by hard impingement.[21,22] This happens when the growth

of a bainitic sub-unit is hindered by another bainitic sheaf or by a prior austenite grain boundary. Hard impingement is more frequent when prior austenite grains are smaller. The restricted growth will cease the lengthening of bainitic laths as formation of new sub-units will be promoted. Moreover, lengthening rate is solely determined by the diffusion of carbon from austenite and rate of formation of sub-units.[23] Now, consider a case at time t_1 when bainite laths are growing as shown in Figure 9(a). After some time, lengthening of the laths ceases due to hitting an austenite grain boundary or by impingement with other laths for a smaller grain size whereas laths continue to lengthen when grains are bigger as shown in Figure 9(b). Once lengthening stops (Figure 9(c)), thickening of laths can be a way to continue transformation in smaller prior austenite grains. Thickening of laths by sidewise
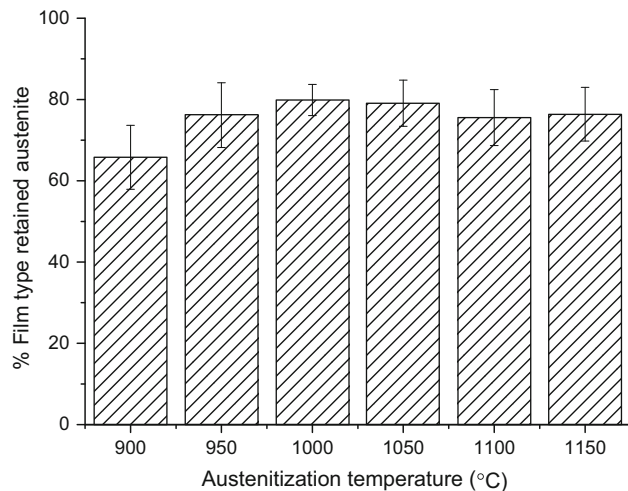
Fig. 7—Percentage of film type retained austenite in specimens with different prior AGS.
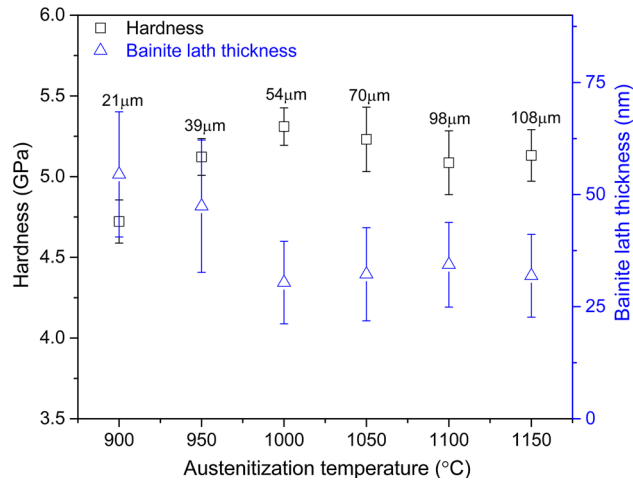

Fig. 8—Bainitic lath thickness and hardness as a function of austenitization temperature. The value above each data point represents the respective prior austenite grain size at given austenitization temperature.

nucleation and growth of new sub-units (sub-unit mechanism) has been reported in other studies.[14] This thickening can continue as long as the chemical driving force is available for bainitic transformation when the specimens are held at that temperature for sufficient time. This is consistent with our findings of similar volume fraction of bainite irrespective of prior AGS when isothermal transformation was done for 8 h as shown in Figure 5.

The above model attempts to explain the formation of thicker bainite laths in small grain size of austenite when the austenitization temperature is kept below 1000 °C and kinetics is growth limited. However, specimens austenitized above this critical temperature showed finer and comparatively longer bainitic laths owing to unrestricted growth of bainitic laths for longer times than for specimens with finer AGS.

The retained austenite in the microstructure has the potential of enhancing the work-hardening ability of steels by undergoing stress or strain assisted phase transformation. This may provide the much-needed ductility in specimens with thinner laths and higher strength. In the current study, large fraction of blocky retained austenite along with discontinuous and thick bainite sheaves is observed in specimens with finer AGS. The growth of these laths is restricted due to impingement of sheaves within carbon saturated austenite regions as well as other sheaves thereby leading to large islands of austenite.[5] It has been reported that film type retained austenite has high carbon content and hence plastic deformation is accommodated in large strain range leading to enhanced ductility by transformation induced plasticity.[24] However, blocky type retained austenite has low carbon and in turn low mechanical stability therefore, the strain induced transformation occurs at early stages of deformation. The percentage of film type retained austenite is higher for specimens austenitized at or above 1000 °C as shown in Figure 7.

The hardness of nanostructured bainite is primarily determined by: (i) bainite volume fraction (V_b) and (ii) bainite lath thickness (t). Bainite volume fraction is a function of carbon content as well as the isothermal temperature and holding time during bainitic transformation. As seen in Figure 5, no appreciable change in volume fraction of bainite is observed in different prior AGS of specimens. However, there is significant variation observed in the lath thickness with a change in prior AGS. Therefore, it is the most critical determinant of hardness in all the specimens. In Figure 8, as the lath thickness decreases, there is smaller mean free path for dislocation to glide and hence the hardness is expected to increase. Specimens of prior AGS higher than 54 μm show comparable hardness of 5.3 GPa owing to similar bainitic lath thickness. Specimens with a prior AGS smaller than 54 μm show degradation in hardness due to coarsening of bainitic laths. However, specimens austenitized at 950 °C, 1100 °C, and 1150 °C shows similar hardness as the ratio of volume fraction of bainite to lath thickness is similar for above conditions.

V. CONCLUSION

NB steels were prepared from specimens with different AGS after isothermal holding for sufficient time at 300 °C to transform the austenite to the maximum possible predicted by T_0' line. Hence, all the specimens had similar amounts of bainitic ferrite and retained austenite. The morphology of the bainitic laths and retained austenite was significantly different between the specimens with low vs high prior AGS. Specimens with lower prior AGS resulted in higher volume fraction of blocky austenite and thicker bainitic sheaves resulting in poor hardness. Smaller prior AGS hinders growth of bainitic laths through grain boundary impingement and also possibly by intersection of non-parallel laths suggesting growth-limited kinetics of transformation. Lateral growth of bainitic sheaves after longitudinal growth impediment is thought to be the most probable reason for the thickening of bainite. Increasing the prior AGS resulted in finer bainitic ferrite that results in high
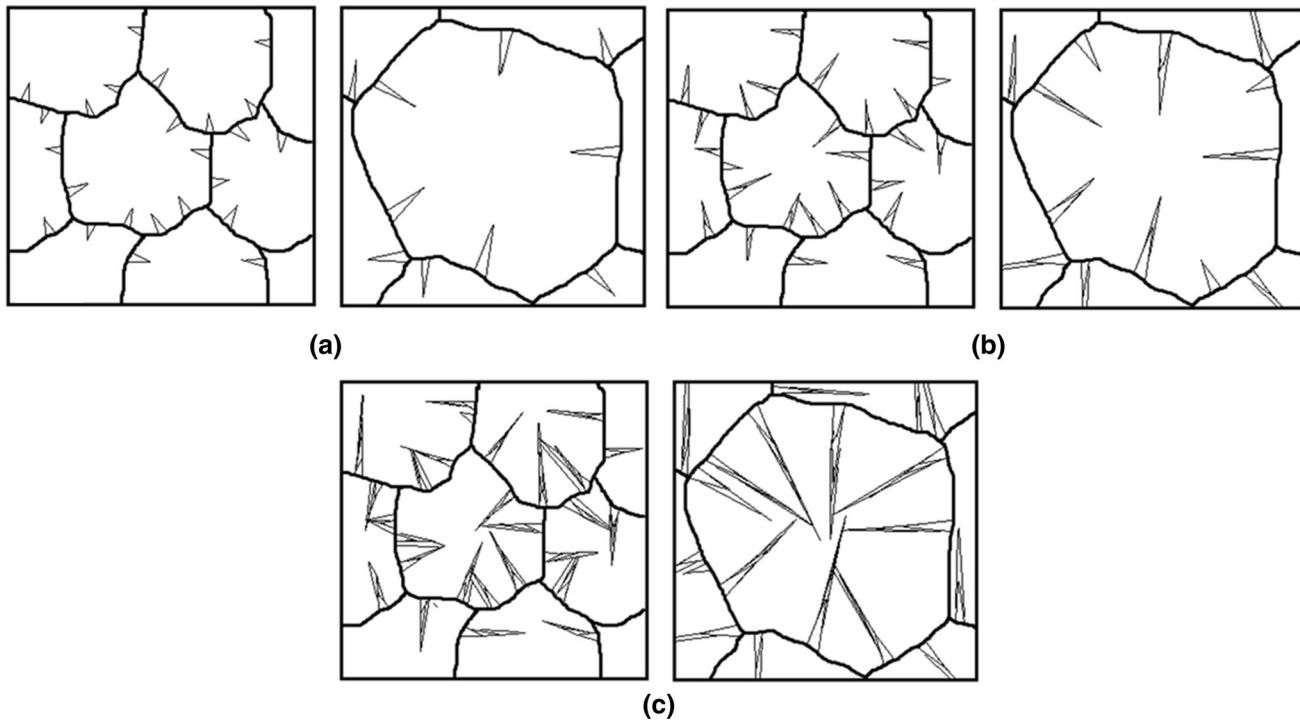
Fig. 9—Schematic illustrating the nucleation and growth of bainite laths with increasing time ($t_1 < t_2 < t_3$) in a fine (left) and coarse (right) austenite grain. (*a*) At t_1: lengthening of sub-units. (*b*) At t_2: impingement of sheaf with grain boundary and other sheaves. (*c*) At t_3: thickening of laths through sub-unit mechanism.

hardness and owing to the higher volume fraction of film-like retained austenite may result in enhanced impact toughness. However, the morphology and hence the hardness did not change significantly as the prior AGS was increased beyond 54 μm.

REFERENCES

1. C. Garcia-Mateo, F.G. Caballero, and H.K.D.H. Bhadeshia: *ISIJ Int.*, 2003, vol. 43, pp. 1821–25.
2. F.G. Caballero and H.K.D.H. Bhadeshia: *Curr. Opin. Solid State Mater. Sci.*, 2004, vol. 8, pp. 251–57.
3. H.K.D.H. Bhadeshia: *Mater. Sci. Technol.*, 2005, vol. 21, pp. 1293–1302.
4. C. García-Mateo, F.G. Caballero, and H.K.D.H. Bhadeshia: *Mater. Sci. Forum*, 2005, vols. 500–501, pp. 495–502.
5. H.K.D.H. Bhadeshia: *Proc. R. Soc. A Math. Phys. Eng. Sci.*, 2010, vol. 466, pp. 3–18.
6. C. Garcia-Mateo and F.G. Caballero: *ISIJ Int.*, 2005, vol. 45, pp. 1736–40.
7. F.G. Caballero, H.K.D.H. Bhadeshia, K.J.A. Mawella, D.G. Jones, and P. Brown: *Mater. Sci. Technol.*, 2002, vol. 18, pp. 279–84.
8. C. Garcia-Mateo, F.G. Caballero, and H.K.D.H. Bhadeshia: *ISIJ Int.*, 2003, vol. 43, pp. 1238–43.
9. H.-T. Chang, H.-W. Yen, W.-T. Lin, C.-Y. Huang, and J.-R. Yang: *Int. Heat Treat. Surf. Eng.*, 2013, vol. 7, pp. 8–15.
10. A. Matsuzaki and H.K.D.H. Bhadeshia: *Mater. Sci. Technol.*, 1999, vol. 15, pp. 518–22.
11. F. Hu, P.D. Hodgson, and K.M. Wu: *Mater. Lett.*, 2014, vol. 122, pp. 240–43.
12. T. Jiang, H. Liu, J. Sun, S. Guo, and Y. Liu: *Mater. Sci. Eng. A*, 2016, vol. 666, pp. 207–13.
13. L. Yuan, Q. Liu, H. Li, and B. Gao: *Met. Sci. Heat Treat.*, 2015, vol. 57, pp. 156–60.
14. H.K.D.H. Bhadeshia: *Bainite in Steels*, 2nd ed., Institute of materials, London, 2001.
15. C. García De Andrés, M.J. Bartolomé, C. Capdevila, D. San Martín, F.G. Caballero, and V. López: *Mater. Charact.*, 2001, vol. 46, pp. 389–98.
16. L.C. Chang and H.K.D.H. Bhadeshia: *Mater. Sci. Technol.*, 1995, vol. 11, pp. 874–82.
17. B.D. Cullity: *Phys. Today*, 1957, vol. 10, pp. 50–51.
18. T. Kaneshita, G. Miyamoto, and T. Furuhara: *Acta Mater.*, 2017, vol. 127, pp. 368–78.
19. H. Beladi, V. Tari, I.B. Timokhina, P. Cizek, G.S. Rohrer, A.D. Rollett, and P.D. Hodgson: *Acta Mater.*, 2017, vol. 127, pp. 426–37.
20. H.K.D.H. Bhadeshia and J.W. Christian: *Metall. Trans. A.*, 1990, vol. 21, pp. 767–97.
21. D.Q. Kong, Q.S. Liu, and Z.J. Dong: *J. Iron Steel Res. Int.*, 2013, vol. 20, pp. 45–49.
22. L.C. Chang and H.K.D.H. Bhadeshia: *Mater. Sci. Technol.*, 1996, vol. 12, pp. 233–36.
23. G.R. Purdy and M. Hillert: *Acta Metall.*, 1984, vol. 32, pp. 823–28.
24. C. García-Mateo and F.G. Caballero: *Mater. Trans.*, 2005, vol. 46, pp. 1839–46.